SCIENCE CHINA
Technological Sciences

• Article •

September 2016 Vol.59 No.9: 1407–1412
doi: 10.1007/s11431-016-6102-6

Full-solution-processed high mobility zinc-tin-oxide thin-film-transistors

ZHANG YunGe, HUANG GenMao, DUAN Lian*, DONG GuiFang, ZHANG DeQiang & QIU Yong*

Key Lab of organic Optoelectronics & Molecular Engineering of ministry of Education, Department of Chemistry, Tsinghua University, Beijing 100084, China

Received January 23, 2016; accepted March 11, 2016; published online August 10, 2016

The full solution-processed oxide thin-film-transistors (TFTs) have the advantages of transparency, ease of large-area fabrication, and low cost, offering great potential applications in switching and driving fields, and attracting extensive research interest. However, the performance of the solution-processed TFTs is generally lower than that of the vacuum-deposited ones. In this article, the full-solution processed TFTs with zinc-tin-oxide (ZTO) semiconductor and aluminium (Al_2O_3) dielectrics were fabricated, and their mobilities in the saturation region are high. Besides, the effect of the Al_2O_3 dielectrics' preparation technology on ZTO TFTs' performance was studied. Comparing the ZTO TFTs using the spin-coated Al_2O_3 dielectrics of 1–4 layers, the ZTO TFT with 3-layer Al_2O_3 dielectrics achieved the optimal performance as its field-effect carrier mobility in the saturation region is 112 cm^2/V s, its threshold voltage is 2.4 V, and its on-to-off current ratio is 2.8×10^5. This is also the highest reported carrier mobility of the solution-processed ZTO TFTs.

solution-processed, ZTO TFT, Al_2O_3, preparation technology

Citation: Zhang Y G, Huang G M, Duan L, et al. Full-solution-processed high mobility zinc-tin-oxide thin-film-transistors. Sci China Tech Sci, 2016, 59: 1407–1412, doi: 10.1007/s11431-016-6102-6

1 Introduction

The thin film transistors (TFTs) based on the solution-processed metal oxide semiconductors have attracted increasing research interest as switching and driving components for the next generation displays because of their excellent properties, such as high optical transparency, good electrical performance, and robust chemical stability [1–4]. Moreover, compared with the complex and expensive vacuum methods, the solution process is simple, low-cost, ease of achieving both composition control and large areas. Over the past decades, significant progress has been accomplished in the solution-processed TFTs using various metal oxide semiconductors, such as ZnO [5,6], In_2O_3 [7], ZTO [8], IZO [9], and IGZO [10]. However, in comparison with the TFTs processed by the vacuum deposition, they still show considerably low field effect mobility due to the defects in the films such as organic residues and pinholes. In 2005, Fortunato et al. summarized the performances of ZnO TFTs fabricated by various methods: the field effect mobility of the sol-gel processed ZnO TFT is 0.2 $cm^2\ V^{-1}\ s^{-1}$, while that of the radio-frequency magnetron sputtered ZnO TFT is over 20 $cm^2\ V^{-1}\ s^{-1}$ [11]. Although impressive progress has been made in promoting the solution-processed TFTs' performance in the last few years, generally they are still inferior to the vacuum processed TFTs.

Not only the semiconductors but also the dielectrics are essential to the TFTs. The kinds and fabrication methods of

*Corresponding authors (email: duanl@mail.tsinghua.edu.cn; qiuy@mail.tsinghua.edu.cn)

the dielectrics have much effect on the chemical composition, capacitance per area (C_i), and roughness of the dielectrics films, which will influence the performance of the TFTs. Using high-k dielectrics that can offer higher C_i, the TFTs can have a larger driving current under a lower operating voltage. The current research on the solution-processed dielectrics has mainly focused on high-k dielectrics, such as Y_2O_3 [12], La_2O_3, HfO_2 [13], ZrO_2 [14], Al_2O_3 [15,16], and their complexes. In particular, Al_2O_3 has been extensively studied, for it has the merits of high relative permittivity (6–10), large band gap (8.7 eV), ease of forming the amorphous phase, nontoxic, and inexpensiveness [17]. In 2013, Nayak et al. [16] reported the performance of the solution-processed indium oxide (In_2O_3) TFTs using AlO_x films annealed at different temperatures as the gate dielectrics. When the precursor $AlCl_3$ annealed at a lower temperature, the resulted AlO_x films showed higher amount of Al-OH groups which can facilitate the oxidation of the In_2O_3, leading to improved device performance. The In_2O_3 TFT with AlO_x film annealed at 350°C exhibited high performance with a field-effect mobility of 127 cm^2/V s, a V_{on} of 0.1 V and an I_{on}/I_{off} ratio of 10^6. In 2009, Pal et al. [18] used the sol-gel-derived sodium beta-alumina (SBA) as the gate dielectrics, which has mobile sodium ions in the lattice planes and requires a high annealing temperature (830°C) for the crystalline formation. The solution-processed ZTO TFT using SBA as gate dielectrics showed a high electron mobility of 28 cm^2/V s with a V_T of 0 V, and an I_{on}/I_{off} ratio of 2×10^4. In 2013, Park et al. added H_2O_2 into the ionic Al_2O_3 precursor solution. The annealed film contains NO_3^- that facilitates the adsorption of H_2O by the electrostatic force, and the H^+ from the adsorbed H_2O remarkably induces a high capacitance by the formation of an electrical double layer. Using the NO_3^- coordinated amorphous Al_2O_3 dielectrics, the TFT based on spin-coated Li–ZnO and In–ZnO exhibited a high field-effect mobility of 46.9 and 44.2 $cm^2\ V^{-1}\ s^{-1}$, respectively, and an I_{on}/I_{off} ratio of 4.64×10^5 and 3.17×10^4, respectively [19].

In this work, we demonstrated the fabrication of high performance and low-voltage operated TFTs using solution processed ZTO as the semiconductor layer and Al_2O_3 of different layers as the gate dielectrics at the maximum preparation temperature of 450°C. We found that the Al_2O_3 film became smoother as its spin-coating times increased from 1 time to 4 times. The ZTO TFT based on Al_2O_3 of 3 layers has the optimal comprehensive performance with a field-effect mobility of 112 cm^2/V s, a threshold voltage of 2.4 V, and an on-to-off current ratio of 2.8×10^5.

2 Experimental

All the reagents, including aluminum nitrate nonahydrate ($Al(NO_3)_3\cdot9H_2O$, 99%), zinc acetate dehydrate ($Zn(CH_3COO)_2\cdot2H_2O$, 98%), tin(II) chloride ($SnCl_2$, 99.5%), 2-methoxyethanol ($CH_3OCH_2CH_2OH$, AR) and ethanolamine ($NH_2CH_2CH_2OH$, AR) were purchased from Alfa Aesar and used without additional purification.

1) Precursor solution preparation. The Al_2O_3 precursor solution was prepared by dissolving 1.88 g $Al(NO_3)_3\cdot9H_2O$ in 10 mL 2-methoxyethanol at a concentration of 0.5 mol/L. The as-prepared solution was stirred rigorously at room temperature for 4 h, yielding a clear transparent solution. The ZTO precursor solution was prepared on the basis of our laboratory's previous experiments [20]: 0.49 g $Zn(CH_3COO)_2\cdot2H_2O$ (0.225 mol/L) and 0.43 g $SnCl_2$ (0.225 mol/L) were dissolved in 10 mL 2-methoxyethanol, and then 1 mL $NH_2CH_2CH_2OH$ was added as the stabilizing agent to improve the solubility of the salts. The solution was stirred rigorously at room temperature for 2 h, yielding a colorless transparent solution. Before spun-coating, the deionized water (1.67 mol/L) was added into the ZTO precursor solution, and the generated white precipitate was dissolved after shaking the solution.

2) Transistor fabrication. The bottom-gate, top-contact (BG-TC) transistors were fabricated on the patterned ITO glass substrate which acts as the common gate electrode. Prior to spin coating, the precursor solutions were filtered through 0.22 um nylon syringe filters. The as-prepared Al_2O_3 precursor solution was spun coated onto the ITO glass substrate at 3000 rpm for 30 sec in the nitrogen glove box, followed by baking on a pre-heated hot plate at 220°C for 5 min to evaporate the solvent. The spin coating-baking cycle was repeated several times to obtain Al_2O_3 films with different thicknesses; then the film was thermal annealing at 450°C for 30 min in the air to generate Al_2O_3. The hydrous ZTO precursor solution was spun coated onto the Al_2O_3 film at 3000 rpm for 30 s, followed by heating on a pre-heated hot plate at 180°C for 5 min in the air (the air humidity was around 50%). Next, the hot plate was heated to 450°C with a rate of 30°C/min, and stayed at 450°C for 30 min to complete the conversion process. Last, the fabrication of the ZTO TFTs was completed with the thermal evaporation of 80 nm-thick Silver (Ag) top source/drain (S/D) electrodes through the shadow mask. The length and width of the channels were 90 and 1350 μm, respectively.

3) Characterization. The thermal property of the $Al(NO_3)_3\cdot9H_2O$ crystals was measured by thermo gravimetric analysis (TGA) and differential thermal analysis (DTA) using a TGA analyzer (TA Instruments, Q5000 IR) in nitrogen with a heating rate of 10°C/min. The crystallinity of the Al_2O_3 films was determined by X-ray diffraction (XRD, D/max-IIIA 3KW, Cu-Ka). The surface roughness of the Al_2O_3 films was analyzed by using an atomic force microscope (AFM, Seiko, SPA400). The thickness of the Al_2O_3 films was characterized by an ellipsometer (EPI, SopraGES5). The length and width of the channels were measured by an optical microscopy (Olympus, BX51M). The capacitance-frequency of the Al_2O_3 films was analyzed by an impedance meter (Agilent, 4294A). The electrical

properties of the ZTO TFTs were characterized in the atmosphere at room temperature using a Keithley 4200 semiconductor parameter analyzer, and no encapsulation layer, or any type of protective layer was applied over the channel region.

3 Results and discussion

To investigate the thermal decomposition process of $Al(NO_3)_3{\cdot}9H_2O$, the TG-DTA measurement was performed and the results are shown in Figure 1(a). Gradual weight loss was observed up to 400°C, which originated from the evaporation of the coordinated water and the decomposition of nitrate groups. Thus, the annealing temperature of 450°C is high enough to generate Al_2O_3 completely.

The XRD measurement was taken to clarify the amorphous phase of the Al_2O_3 film. The Al_2O_3 film was spun coated onto the silicon substrate which was ultrasonic cleaned in ethanol, toluene, acetone, and isopropanol sequentially, and then was cleaned in ultraviolet cleaning machine for 10 min. The results are shown in Figure 2, which indicates that the Al_2O_3 film is amorphous, as the peak at 69.1° belongs to the Si(100). For gate dielectrics, the amorphous phase is preferred for it can effectively prevent the leakage current arising from the structure defects and the carrier tunneling induced by the crystalline grain boundaries [21].

Figure 3 shows the tapping-mode atomic force microscopy (AFM) surface topography images for 1–4-layer Al_2O_3 films spun coated on the silicon substrates. All films' surfaces are found to be uniform and smooth. The root-mean-square roughness (R_{RMS}) of the 1–4-layer Al_2O_3 films is 0.15, 0.13, 0.10, and 0.09 nm, respectively, showing that the Al_2O_3 film becomes smoother as its layer increases. The smooth surface is beneficial to form a good interface between the Al_2O_3 layer and the ZTO layer, which favors the electron transfer in the ZTO layer. The ellipsometer results indicate that the Al_2O_3 film's thickness increases linearly as the layer increases from 1 to 4. The detailed data of AFM and the ellipsometer results are summarized in Table 1.

To investigate the dielectric behaviors of the 1–4-layer Al_2O_3 films, the capacitance vs. frequency characteristic was obtained by Agilent 4294A from the ITO/Al_2O_3/Ag structure, as is shown in Figure 4. The capacitance per area decreased as the thickness increased. The Al_2O_3 films of 1–4 layers show the capacitance per area of 980, 556, 192, and 177 nF/cm^2, respectively, at 1 kHz. In addition, they showed a lower value of capacitance at a higher frequency. In general, the capacitance of the conventional dielectric films shows a constant value when the frequency is lower than 1 MHz, and decreases at a super high frequency [22].

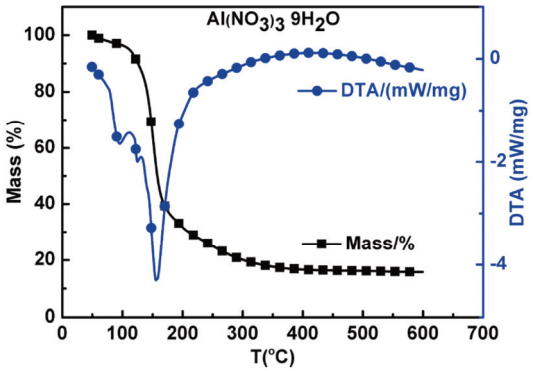

Figure 1 (Color online) TG-DTA for $Al(NO_3)_3{\cdot}9H_2O$ crystals.

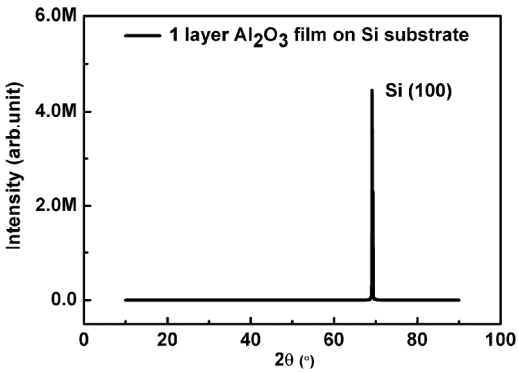

Figure 2 XRD for 1 layer Al_2O_3 film on Si substrate.

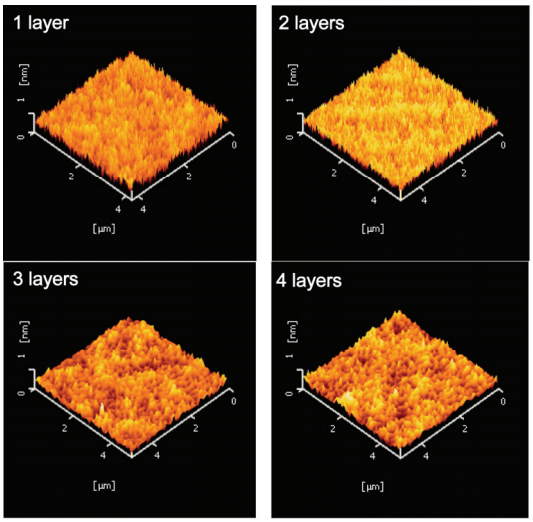

Figure 3 (Color online) AFM for 1–4 layers Al_2O_3 films on Si substrate.

Table 1 AFM and thickness data for the 1–4 layers Al_2O_3 films on the Si substrate

The layer of Al_2O_3 films	thickness d (nm)	P-V (nm)	RMS (nm)
1	40	2.2	0.15
2	89	1.4	0.13
3	131	0.98	0.10
4	187	0.95	0.09

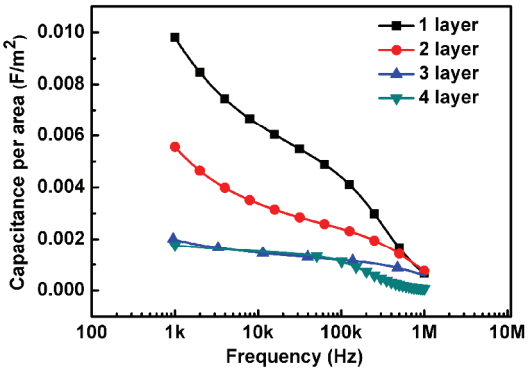

Figure 4 (Color online) Capacitance-frequency for the 1–4-layer Al_2O_3 films by the ITO/Al_2O_3/Ag structure.

However, the solution-processed Al_2O_3 films showed frequency dependent dielectric behaviors from 1 kHz to 1 MHz. These variations may be resulted from the mobile ion, such as H^+, in Al_2O_3 films. Compared with the 1 and 2-layer Al_2O_3 films, the capacitance of 3 and 4-layer Al_2O_3 films is more stable as the frequency increases, which is good for gate dielectrics.

In order to investigate the potential impact of the Al_2O_3 film morphologies on the electron transport in the solution-processed ZTO films, we have fabricated the bottom-gate top-contact structure TFTs with 1–4-layer Al_2O_3 films, named device A, B, C, and D, respectively. The thickness of the ZTO layer was found to be 30 nm by the ellipsometer. Device A has no field effect performance, perhaps because the 1 layer spin-coated Al_2O_3 film has too many defects (such as pinholes and pores) that cannot be effective gate dielectrics. For device B, C, and D, the illustration of the device structures and their electrical characteristics are shown in Figure 5.

To avoid overestimating the electron mobility, we use the capacitance values of the Al_2O_3 films at 1 kHz [19]. The

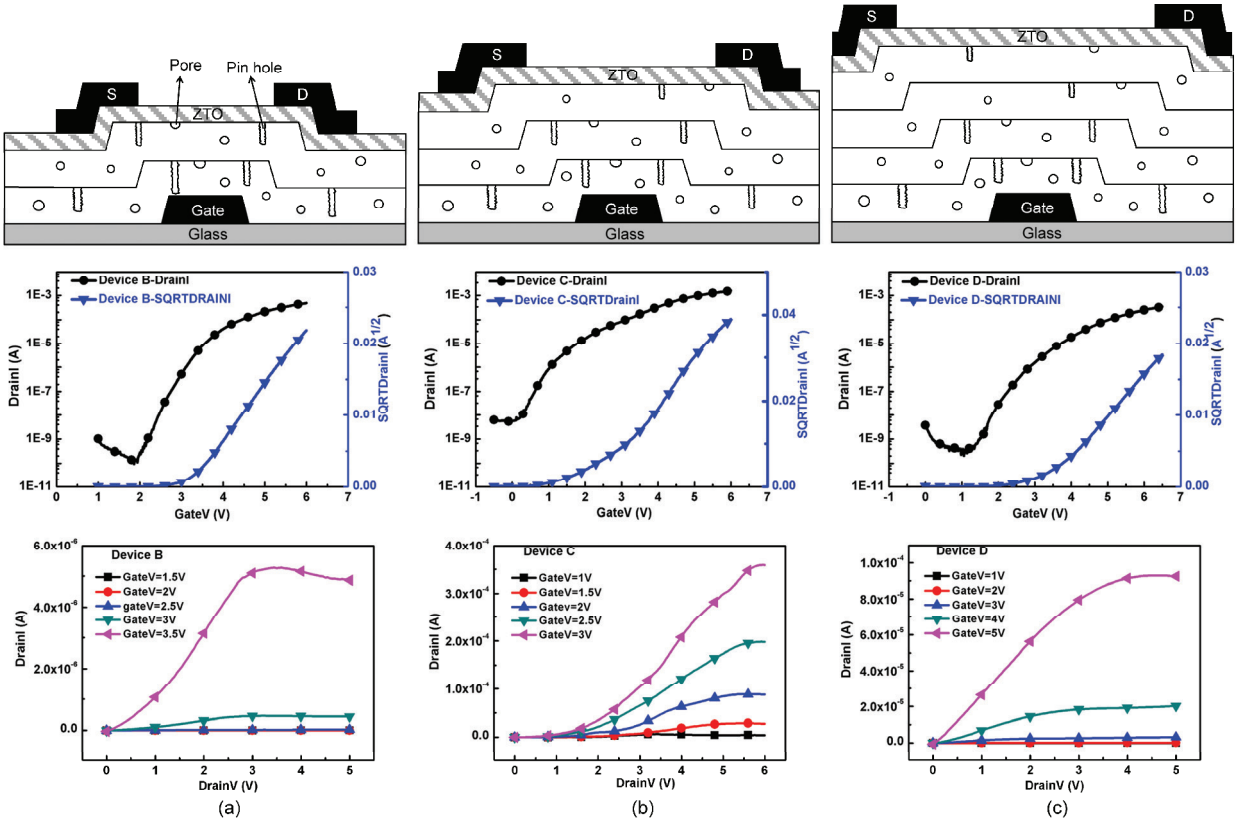

Figure 5 (Color online) The device structures, transfer characteristics (Drain V=3 V) and output characteristics of device B, C, and D.

Table 2 The electrical characteristics data for device A–D

Device	Mobility (cm^2/V s)	V_T (V)	I_{on}/I_{off}	S (V/decade)	$N_\square$ (/cm^2 eV)
A-1 layer Al_2O_3	–	–	–	–	–
B-2 layer Al_2O_3	20	3.2	5.1×10^6	0.27	1.26×10^{13}
C-3 layer Al_2O_3	112	2.4	2.8×10^5	0.35	6.00×10^{12}
D-4 layer Al_2O_3	36	3.4	1.6×10^6	0.38	6.01×10^{12}

field-effect mobility in the saturation region was extracted by using the gradual channel approximation:

$$\mu = \frac{2L}{WC_i}\left[\frac{\sqrt{I_D}}{V_G}\right]^2.$$

The performance parameters of device A–D were summarized in Table 2. Generally, more accumulated charge carriers will be induced into thinner dielectrics, which can enhance the apparent carrier mobility as the solution-processed metal-oxide semiconductor usually has many carrier traps. However, in this study, the ZTO TFT with 3-layer Al_2O_3 film possesses the highest mobility (112 $cm^2/V{\cdot}s$, almost 5 times higher than that of the ZTO TFT with 2-layer Al_2O_3 film). Compared with the 3-layer Al_2O_3 film, the 2-layer Al_2O_3 film's surface is rougher, which may lead to more ZTO micro zones in the interface between the dielectric layer and the semiconductor layer, bringing about more trap states. The trap density $N_{\square}$ (including the interface traps and the bulk traps in the semiconductor layer) can be calculated by the equation [23]:

$$S = \frac{kT\ln 10}{e}\left[1+\frac{e^2}{c_i}N_{\square}\right],$$

where S is the subthreshold swing and C_i is the capacitance per area. The trap density $N_{\square}$ of device B is about twice as much as that of device C and D (The $N_{\square}$ of device B, C, and D is 1.26×10^{13}, 0.600×10^{13}, and 0.601×10^{13} $/cm^2\,eV$, respectively). For device D, although its trap density is as low as device C, its carrier mobility is lower than device C for its carrier concentration is lower. The leakage current of device B, C, and D at V_{DS} = 3 V and V_{GS} = 6 V is 6.87×10^{-5}, 1.06×10^{-5}, and 4.72×10^{-5} A, respectively, which is much higher than that of the conventional dielectric SiO_2 ($\sim10^{-10}$ A). That may be resulted from the fact that the semiconductor film is unpatterned and that there probably exist mobile ions such as H^+ in the solution-processed Al_2O_3 films. Compared with device B and D, device C's I_{off} is larger (I_{off} for device B, C, and D is 1.1×10^{-10}, 5.4×10^{-9}, and 2.0×10^{-10} A, respectively) and its V_T is smaller (V_T for device B, C, and D is 3.2, 2.4, and 3.4 V, respectively). Perhaps because the 3-layer Al_2O_3 film contains more mobile ions, which help to generate the conducting channel at a lower voltage and increase the off current as well [19].

4 Conclusion

In conclusion, we have developed full-solution processed ZTO TFTs with Al_2O_3 dielectric on the ITO glass substrates. By changing the Al_2O_3 films' layer from 1 to 4, we demonstrated a ZTO TFT with a very high electron mobility (112 $cm^2/V\ s$). In the AFM tests, the surfaces of the 3-layer-Al_2O_3 film and 4-layer-Al_2O_3 film are smoother than those of 1 layer-Al_2O_3 film and 2-layer-Al_2O_3 film, which is advantageous to form fewer interface trap states, improving the electron transfer. These results demonstrate that the solution-processed ZTO TFT can exhibit higher mobility than that via the conventional approaches, and that the solution processed Al_2O_3 dielectric could be applicable to the electronics of the next generation.

This work was supported by the National Natural Science Foundation of China (Grant No. 21161160447).

1 Park J S, Maeng W J, Kim H S, et al. Review of recent developments in amorphous oxide semiconductor thin-film transistor devices. Thin Solid Films, 2012, 520: 1679–1693
2 Fortunato E, Barquinha P, Martins R. Oxide semiconductor thin-film transistors: A review of recent advances. Adv Mater, 2012, 24: 2945–2986
3 Si Joon K, Seokhyun Y, Hyun Jae K. Review of solution-processed oxide thin-film transistors. Jpn J Appl Phys, 2014, 53: 02BA02
4 Thomas S R, Pattanasattayavong P, Anthopoulos T D. Solution-processable metal oxide semiconductors for thin-film transistor applications. Chem Soc Rev, 2013, 42: 6910–6923
5 Ong B S, Li C, Li Y, et al. Stable, solution-processed, high-mobility ZnO thin-film transistors. J Am Chem Soc, 2007, 129: 2750–2751
6 Meyers S T, Anderson J T, Hung C M, et al. Aqueous inorganic inks for low-temperature fabrication of ZnO TFTs. J Am Chem Soc, 2008, 130: 17603–17609
7 Kim H S, Byrne P D, Facchetti A, et al. High performance solution-processed indium oxide thin-film transistors. J Am Chem Soc, 2008, 130: 12580–12581
8 Zhao Y, Duan L, Dong G, et al. High-performance transistors based on zinc tin oxides by single spin-coating process. Langmuir, 2012, 29: 151–157
9 Banger K K, Yamashita Y, Mori K, et al. Low-temperature, high-performance solution-processed metal oxide thin-film transistors formed by a 'sol–gel on chip' process. Nat Mater, 2010, 10: 45–50
10 Rim Y S, Chen H, Kou X, et al. Boost up mobility of solution-processed metal oxide thin-film transistors via confining structure on electron pathways. Adv Mater, 2014, 26: 4273–4278
11 Fortunato E, Barquinha P, Pimentel A, et al. Recent advances in ZnO transparent thin film transistors. Thin Solid Films, 2005, 487: 205–211
12 Song K, Yang W, Jung Y, et al. A solution-processed yttrium oxide gate insulator for high-performance all-solution-processed fully transparent thin film transistors. J Mater Chem, 2012, 22: 21265–21271
13 Choi J H, Mao Y, Chang J P. Development of hafnium based high-k materials—A review. Mat Sci Eng R Reports, 2011, 72: 97–136
14 Jang J, Kitsomboonloha R, Swisher S L, et al. Transparent high-performance thin film transistors from solution-processed SnO_2/ZrO_2 gel-like precursors. Adv Mater, 2013, 25: 1042–1047
15 Xia D X, Xu J B. High mobility and low operating voltage ZnGaO and ZnGaLiO transistors with spin-coated Al_2O_3 as gate dielectric. J Phys D Appl Phys, 2010, 43: 442001
16 Nayak P K, Hedhili M N, Cha D, et al. High performance In_2O_3 thin film transistors using chemically derived aluminum oxide dielectric. Appl Phys Lett, 2013, 103: 033518
17 John R. High dielectric constant gate oxides for metal oxide Si transistors. Rep Prog Phys, 2006, 69: 327

18 Pal B N, Dhar B M, See K C, et al. Solution-deposited sodium beta-alumina gate dielectrics for low-voltage and transparent field-effect transistors. Nat Mater, 2009, 8: 898–903
19 Park J H, Kim K, Yoo Y B, et al. Water adsorption effects of nitrate ion coordinated Al_2O_3 dielectric for high performance metal-oxide thin-film transistor. J Mat Chem C, 2013, 1: 7166–7174
20 Zhao Y, Dong G, Duan L, et al. Impacts of Sn precursors on solution-processed amorphous zinc-tin oxide films and their transistors. RSC Adv, 2012 2: 5307–5313
21 Ortiz R P, Facchetti A, Marks T J. High-k organic, inorganic, and hybrid dielectrics for low-voltage organic field-effect transistors. Chem Rev, 2010, 110: 205–239
22 Wilk G D, Wallace R M, Anthony J M. High-κ gate dielectrics: Current status and materials properties considerations. J Appl Phys, 2001, 89: 5243–5275
23 Wolfgang L K, Bertram B. Calculating the trap density of states in organic field-effect transistors from experiment: A comparison of different methods. Phys Rev B, 2010, 81: 035327